INTL JOURNAL OF ELECTRONICS AND TELECOMMUNICATIONS, 2016, VOL. 62, NO. 4, PP. 371-378
Manuscript received September 29, 2016; revised November, 2016. DOI: 10.1515/eletel-2016-0051

Analysis of Object Location Accuracy for iBeacon Technology based on the RSSI Path Loss Model and Fingerprint Map

Damian E. Grzechca, Piotr Pelczar, and Lukas Chruszczyk

***Abstract*—This paper presents analysis of object location accuracy of a mobile device on the basis of the iBeacon technology. The research starts with radio signal strength indicator analysis along the corridor in order to create a path loss model for iBeacon. Two cases are taken into account: line of sight and non-line of sight for model creation. For both cases two tests: Chi-square, Shapiro-Wilk have been performed. It has also been checked if the HCI (Host Controller Interface) is a source with a memory. Acquired data have been filtered with different type of filters, e.g. median, moving average and then compared. Next, the authors evaluated the indoor positioning trilateration algorithms with the use of created model for exemplary hall. The RSSI map (radiomap) was created and the logarithm propagation model was designed. The logarithmic model estimated distance with average error 1.09m for 1 – 9m and 1.75m for 1-20m and after trilateration, the positions with average error 2.45m was achieved. A statistical analysis for acquiring data led to the final conclusion which enhanced knowledge about positioning based on the popular iBeacon technology.**

***Keywords*—bluetooth, indoor environments, navigation, radio link, radiowave propagation.**

I. Introduction

THE customer's positioning is important in relatively wide indoor areas like museums where localization and pathway creation may be crucial. Moreover, observation and analysis of the customer behavior in the hipermarket may improve different actions (discounts) addressed to a particular group of people.

Many indoor positioning techniques [1]–[5] have been proposed for mobile devices and for more specified, dedicated hardware. Some of them are based on custom hardware utilizing Bluetooth Classic [6], [7], especially in scanning phase to obtain RSSI (Radio Signal Strength Indicator) or Link Quality [8]–[10]. Unfortunately, Bluetooth Classic scanning phase is energy-consuming, because obtaining Link Quality metrics requires devices connection. The Bluetooth 4.0 (also known as Low Energy or BLE-Bluetooth Low Energy) was released in 2011 and today, it is widely supported by smartphone vendors. This has opened a new opportunity for identification of devices and obtaining RSSI in the lower energy cost way. BLE beacon devices broadcasts short packets in specific interval, which gives a new possibility to use beacon standard in a wide range for a population of people holding these devices in their pockets.

In 2013, Apple released iBeacon standard [7], [11], [12] as a proximity location method, which utilizes Bluetooth 4.0 Generic Attribute (GATT) profile and standardized frame data contents. The iBeacon standard by Apple enabled mobile devices to recognize Beacon tags by receiving Bluetooth signals from them. In addition, the Eddystone standard was proposed by Google in order to extend the iBeacon, which are both widely supported by mobile device vendors in hardware and in software by implementing iBeacon and Eddystone into operating systems running on these devices. Then, many vendors started producing low-cost hardware broadcasting beacon frames, which h can be discovered by mobile devices. This standard is natively supported on Apple iOS mobile devices, also, it is easy to carry out in every platform which delivers access to Bluetooth Host Controller Interface (HCI), such as on devices running on Android or Windows Phone. The iBeacon frame is sent over the air with an interval of about 350ms. Its structure is presented in Figures 1 and 2. In Figure 1, the Bluetooth device is sending an *advertisement type packet* without establishing a connection, that is, a device invites to connect by sending some data but rejects incoming connections.

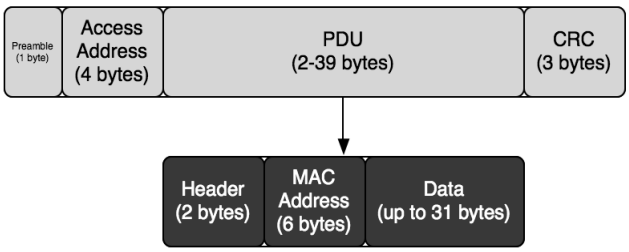

Fig. 1. iBeacon Advertisement Bluetooth packet structure.

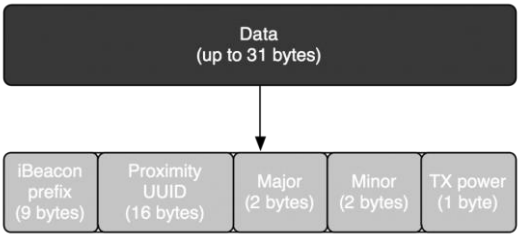

Fig. 2. iBeacon Advertisement packet data payload contents.

While iBeacon became popular, in 2015, Google released extended specification of the standard called Eddystone. The standard is very similar to the iBeacon in the way it works, but

This work was partially supported by Ministry of Science and Higher Education.

D. Grzechca is with the Faculty of Automatic Control, Electronics and Computer Science, Silesian University of Technology, Gliwice, Poland, (e-mail: dgrzechca@polsl.pl).

P. Pelczar is with the Faculty of Automatic Control, Electronics and Computer Science, Gliwice, Poland (e-mail: me@athlan.pl).

L. Chruszczyk is with the Institute of Electronics, Silesian University of Technology, Gliwice, Poland, (e-mail: lch@polsl.pl).

the frame content is different. Eddystone (so far) assumes three types of data frame [12]:

1) Eddystone-UID (User IDentifier) which is the same as beacon frame, the data packet is filled by 16 byte beacon ID (10 bytes namespace ID and 6 byte instance ID),

2) Eddytone-URL filled by encoding and shortened URL that can be opened by mobile devices without accessing the cloud to relate broadcasted ID by beacon to assigned URL. This URL is directly from the source IoT (Internet of things) or Physical Web URL. Mobile customers can open real online application found under this URL or only run some designed custom URI protocol in the operating system.

3) Eddytsone TLM (also known as Telemetry) allows devices to send small pieces of data such as temperature, battery voltage and so on. Eddystone extends the iBeacon standard, enabling users to send small pieces of data. The beacon can transmit different types of frames over time.

Power-based positioning techniques rely on the signal attenuation property of the radio wave propagation to estimate distance from wave emitter [8], [10], [13], [14]. There are two common approaches to determine an object's position. One is creating the radiomap of a room in offline (static) phase, this means there are many RSSI once-collected samples in many points stored in the database and in the online phase, when an object collects samples of RSSI to determine its position, some nearest-neighbor algorithms determine the object's position comparing this to samples from the database [4], [15]. Another one employs surveying to build path-loss signal model that estimates the distance from emitter based on signal-strength. By knowing three or more distances, the trilateration algorithms can be applied in order to obtain the final position of an object.

In the case of changing environment the another way to improve results is using adaptive distance estimation methods by continuously computing reference $RSSI_0$ values between reference nodes at d_0 distances instead of creating static calibration. In [2] authors reduced distance estimation error from 10% to 4%. For this research, the Logarithmic Distance Path-Loss estimation model was tuned by the simplex algorithm to determine distance based on RSSI. Additionally, radiomaps were created for all accessible beacons in a number of points in the room. Created model were used to determine distances from beacons in each radiomap point and trilateration algorithms were used to compute the final position. Estimated distances and positions were compared to radiomap data in order to designate errors and measure the effectiveness of the proposed approach. This paper is thus organized as follows: Section 2 and 3 introduce the path loss model and trilateration algorithms, respectively. Section 4 describes the data acquisition process and presents fundamental statistical analysis of gathered data. Next, Section 5 explains the tuning process; and finally, experimental results are presented in section 6.

II. PATH-LOSS MODEL

There are several path-loss models available to measure the distance from wave emitter by measuring signal strength [6], [8], [16], [17]. Typically, log-distance path loss model was investigated:

$$RSSI = RSSI_0 - 10\gamma \log_{10} \frac{d}{d_0} + X_\sigma \tag{1}$$

where: d is the distance from wave emitter, $RSSI$ indicates the received power [dBm] (signal strength), $RSSI_0$ is power measured in the distance d_0, X_σ is the Gaussian random noise variables with mean value of zero and mean variance of σ. The coefficient γ represents the path-loss exponent defining the rate at which the power falls. In free space, it is equal to 2, but in real environment, it depends on many elements, such as surrounding objects, wave reflections, scattering, diffraction and signal multipath [3], [13], [18]. The factory was designated in the optimization process by fitting gathered RSSI samples to the model (1). The process gave results from 1 to 1.4 for coefficient γ. Another investigation of the radio channel has been described in [19].

The equation (1) can be rearranged and the distance, d as a function of $RSSI$ was:

$$d = d_0 10^{\frac{RSSI_0 - RSSI + X_\sigma}{10\gamma}} \tag{2}$$

What is important is that estimated d value should be greater than d_0, because the formula is based on on path loss and $RSSI_0$ - $RSSI$ should be greater than 0. There is no sense in making distance estimation for $d < d_0$ in context of path-loss, because in this case, power will increase.

I. TRILATERATION ALGORITHMS

There are two main trilateration algorithms investigated for an unbounded n number of beacons at positions (x_i, y_i) and distances d_i. Both algorithms are described in the following two subsections [3], [20].

A. Algorithm 1 (3.A.)

Denote matrix $B_{n\times 2}$ as reference points and distances vector $R_{n\times 1}$:

$$B = \begin{bmatrix} x_1 & y_1 \\ x_2 & y_2 \\ \vdots & \vdots \\ x_n & y_n \end{bmatrix} \quad R = \begin{bmatrix} d_1 \\ d_2 \\ \vdots \\ d_n \end{bmatrix} \tag{3}$$

One primary reference point is selected $P_r(x_r, y_r)$ at the distance d_r, for example, $B_1(x_1, y_1)$, and matrix $D_{(n-1)\times 2}$ for $I = 1 .. n$ and $I \neq r$ is filled as follows:

$$D = \begin{bmatrix} \vdots & \vdots \\ 2\cdot(x_r - x_i) & 2\cdot(y_r - y_i) \\ \vdots & \vdots \end{bmatrix} \tag{4}$$

Vector $\vec{b}_{(n-1)\times 1}$ for $I = 1 .. n$ and $I \neq r$ is defined as follows:

$$\vec{b} = \begin{bmatrix} \vdots \\ x_r^2 - x_i^2 + y_r^2 - y_i^2 - d_r^2 + d_i^2 \\ \vdots \end{bmatrix} \tag{5}$$

Matrix $Q_{1\times 2}$ indicates the final position of object relative to reference points and distances, by resolving equation:

$$Q = (D^T \cdot D) D^T \cdot \vec{b} \tag{6}$$

B. Algorithm 2 (3.B.)

Pick one primary reference point $P_r(x_r, y_r)$ at the distance d_r, for example, $B_1(x_1, y_1)$, and matrix $H_{(n-1)\times 2}$ for $I = 1 .. n$ and $I \neq r$ is filled as follows:

$$H = \begin{bmatrix} \vdots & \vdots \\ x_i - x_r & y_i - y_r \\ \vdots & \vdots \end{bmatrix} \tag{7}$$

Vector $b_{(n-1)\times 1}$ for $I = 1 .. n$ and $I \neq r$ is defined as:

$$b = \begin{bmatrix} \vdots \\ \frac{1}{2}((x_i - x_r)^2 + (y_i - y_r)^2 - d_i + d_r) \\ \vdots \end{bmatrix} \tag{8}$$

Next, the equation is resolved:

$$\begin{aligned} H \cdot x &= b \\ x &= X^{-1} \cdot b \end{aligned} \tag{9}$$

Where X^{-1} is Moore-Penrose pseudoinverse of X. The final position is defined as matrix Q, after computing:

$$\begin{aligned} Q &= x^T + \begin{bmatrix} x_r & y_r \end{bmatrix} \\ Q &= \begin{bmatrix} x_r \\ y_r \end{bmatrix} \end{aligned} \tag{10}$$

The aforementioned approaches were used to define estimated positions at given points on the radiomap. Both algorithms were compared against input data after distance estimation using the path-loss model in order to measure error-tolerance.

II. Data Acquisition and Analysis

A. Path-loss model creation

In order to create a relatively high precision path loss model, data acquisition and fundamental statistical analysis were applied.

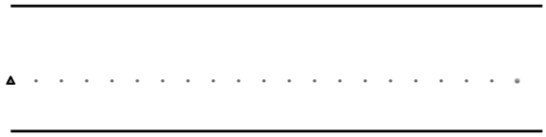

Fig. 3. Data acquisition points (red) from beacon (triangle).

For a single position in the room, a set of 100 RSSI readings per beacon (anchor) was collected. The distance between following points was set to 1m which gave a total of 21 points in a straight line.

$$RSSI_{(p)} = \{RSSI_{(p,1)}, RSSI_{(p,2)}, \ldots, RSSI_{(p,n)}\} \tag{11}$$

where: $RSSI_{(p)}$ - the set of RSSI readings from a beacon in the point p; $RSSI_{(p,n)}$ - the n-th reading from a beacon in the point p

The human body wave power absorbiton was also taken into account – RSSI readings were collected for line-of-sight (LOS) facing towards the beacon and non-LOS directed back to the beacon. The measurements were collected on a 5m wide hallway (presented in Fig. 3) with walls made of two materials: from one side glass (windows) and another side, reinforced concrete. All data ($RSSI_{(p)}$) in the position were aggregated into a single $RSSIM_{(p)}$ value by computing median:

$$\begin{aligned} RSSIM_{(p)} &= RSSI_{\left(p,\frac{n+1}{2}\right)} && \text{for } n \text{ odd} \\ RSSIM_{(p)} &= \frac{1}{2}\left(RSSI_{\left(p,\frac{n}{2}\right)} + RSSI_{\left(p,\frac{n+1}{2}\right)}\right) && \text{for } n \text{ even} \end{aligned} \tag{12}$$

The aggregated $RSSIM_{(p)}$ values and standard deviation $RSSI_{(p,n)}$ over distance (p) is presented in Fig. 4, 5.

The relationship between distance from the beacon and RSSI for both LOS and non-LOS was calculated using Pearson correlation coefficient (4) which gave a value of 90.1%.

$$r_{XY} = \frac{\operatorname{cov}(XY)}{\sigma_X \sigma_Y} \tag{13}$$

where X denotes $RSSIM_{(p)}$ value and Y denotes the distance at point p from the beacon and:

$$\begin{aligned} \bar{x} &= \frac{1}{n}\sum_{i=1}^{n} x_i \quad \bar{y} = \frac{1}{n}\sum_{i=1}^{n} y_i \\ \operatorname{cov}(XY) &= \sum_{i=1}^{n}(x_i - \bar{x})(y_i - \bar{y}) \\ \sigma_X &= \sqrt{\sum_{i=1}^{n}(x_i - \bar{x})^2} \\ \sigma_Y &= \sqrt{\sum_{i=1}^{n}(y_i - \bar{y})^2} \end{aligned} \tag{14}$$

Evidently, the distance from the source has the highest impact on signal intensity. Moreover, there was a weak correlation between standard deviation and distance, even when the input samples was reduced by filtering 20% extreme values with respect to median (Fig. 5). The signal quality indicator cannot rely on this metric.

In equation (1), X_σ is denoted as the Gaussian random noise variables with zero mean and mean variance of σ. The RSSI samples distribution was measured for a distance of 1m (Fig. 6), 3m (Fig. 7), 5m, 7m, 10m, 15m and 20m. The Chi-square statistical test with 5% significance level and Shapiro-Wilk with 5% significance level was ran to ensure, that the RSSI samples have Gaussian distribution. Tests have rejected this hypothesis in several cases, so empirically measured X_σ is a noise with Gaussian distribution (Fig. 7). In this case, it was decided to tune γ path-loss exponent factor and X_σ noise in the model optimization process.

According to Apple documentation for iBeacon standard, the reference $RSSI_0$ value for 1m distance must be assumed (or measured) at first. Fortunately, the acquired samples have Gaussian distribution in this instance, which is important for formula model (1) and X_σ value.

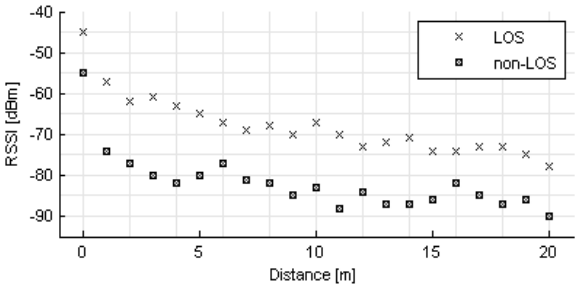

Fig. 4. Median of measured RSSI (LOS and non-LOS).

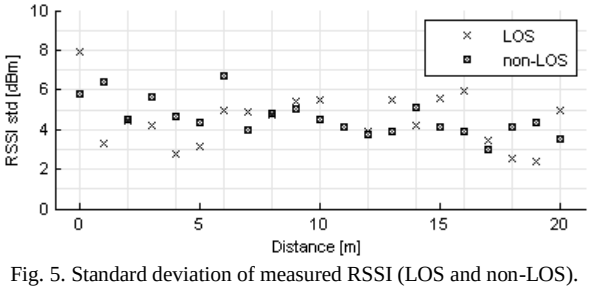

Fig. 5. Standard deviation of measured RSSI (LOS and non-LOS).

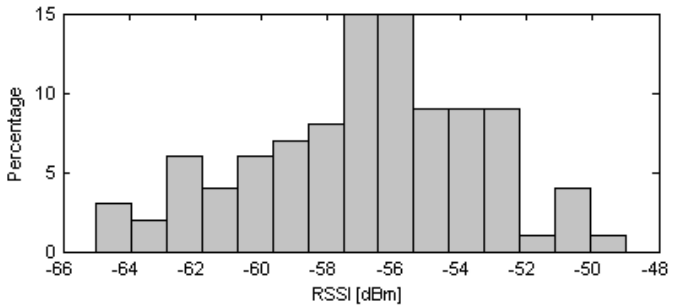

Fig. 6. RSSI distribution on distance 1m.

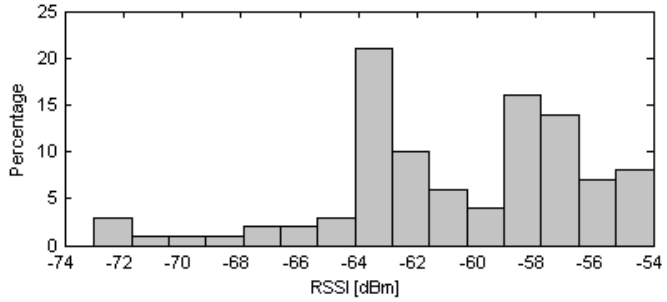

Fig. 7. RSSI distribution on distance 3m.

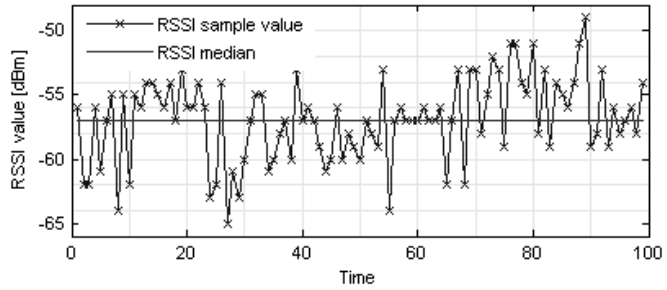

Fig. 8. RSSI samples vs. time on distance 1m.

Another important doubt flows from a source of measurements, that is, HCI (Host Controller Interface). The question is whether the HCI is a source with a memory or it produces random values while being independent of history. In other words, a source stability and the unexpected randomness was investigated. To detect if RSSI samples are time-dependent, the series test was carried out for window size w = 5 and w = 7, which contains sequenced n samples. The test was performed for the whole dataset (100 samples) in one chosen point, where $RSSI_0$ reference value was obtained from d_0 equals to 1m. We performed n-w tests on samples x_1, x_2, … x_{n-w}. All performed tests have rejected hypothesis, this means that samples are time-independent and random RSSI samples obtained over time are presented in Fig. 8.

B. The radiomap creation

The trilateration algorithms (3.A. and 3.B. – described in section 3) position estimation and validation of the tuned model of the radiomap was created for the exemplary room. One hundred RSSI samples from 5 different beacons in each radiomap point were acquired. The radiomap was placed on the 8m × 6m mesh with a gap of 1m (Fig. 9).

$$RSSI_{(p,b)} = \{RSSI_{(p,b,1)}, RSSI_{(p,b,2)}, \ldots, RSSI_{(p,b,n)}\} \quad (15)$$

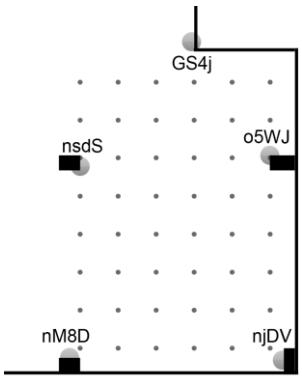

Fig. 9. Data acquisition points (red) from beacons (blue points).

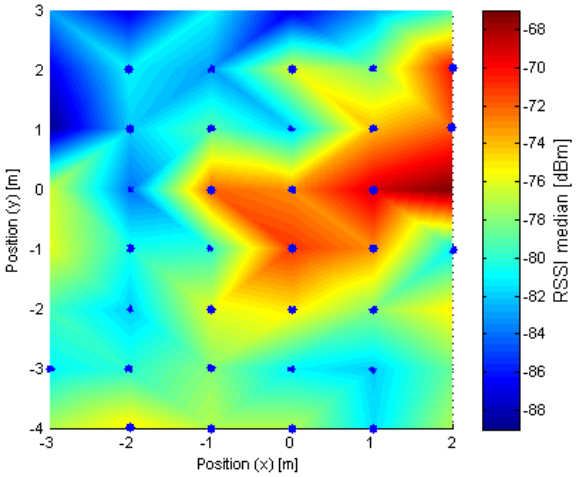

Fig. 10. Radiomap (RSSI mean value) for one beacon device placed in point P(2,0).

where:

- $RSSI_{(p, b)}$ - the set of RSSI readings from beacon b in point p
- $RSSI_{(p, b, n)}$ - the n-th reading from beacon b in point p.

A basic statistic like median for all accessible devices (anchors) in each point was computed. A beacon (an anchor) was mounted under the ceiling (on the top part of the wall to minimize furniture signal absorption) at a height of 2m from the floor, but measurements were collected at the height of 1m, because it seems to be a natural position for smartphones while being used by humans. Exemplary radiomap for one beacon device is presented in Fig. 10.

III. TUNING PATH-LOSS MODEL

Formula (1) path-loss model was tuned by using the data collected (in section 3. A. Matlab) environment has been used for fitting data with model (1). The Nelder-Mead simplex direct search, iterative method (known also as downhill simplex method) against quality function based on MSE of model was used as an unconstrained nonlinear optimization method. The algorithm returns γ = -1.33379 for $RSSI_0$ equals to -56.8687 dBm (the model was compared with the acquired data and results are presented in Fig. 11). Equation (1) was transformed to Equation (2) and the distance based on RSSI was estimated as presented in Fig. 12.

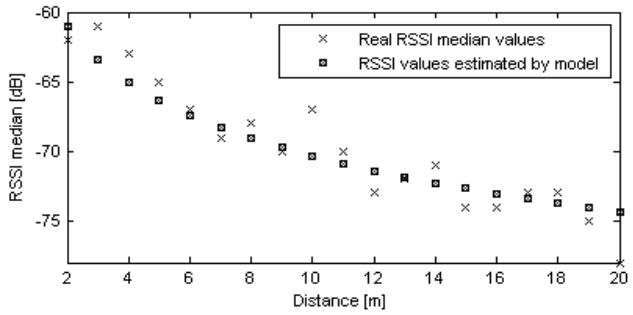

Figure 11. Tuned path-loss model.

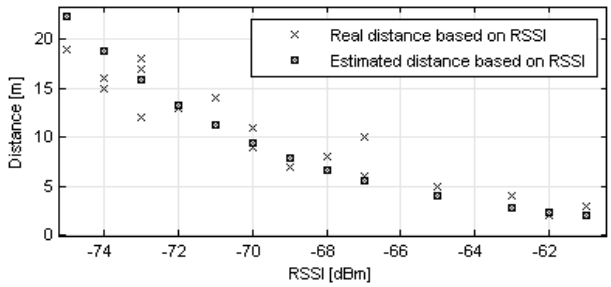

Figure 12. Distance estimated by tuned model compared to real distance.

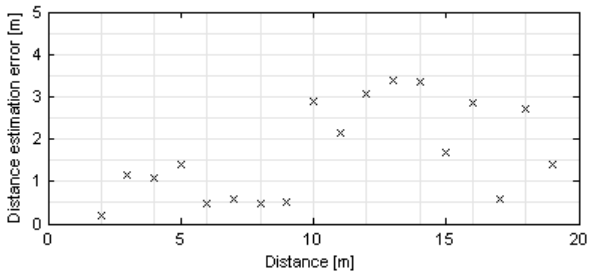

Fig. 13. Error of Distance estimation by tuned model over the distance.

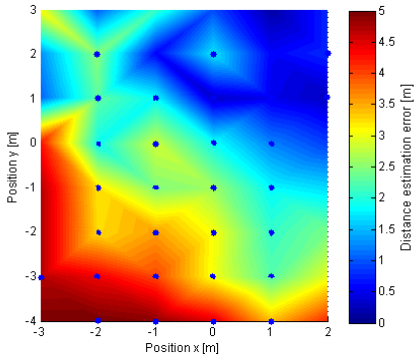

Fig. 14. Distance estimation error for one beacon device placed in point P(2,0).

Fig. 13 presents the error between obtained model and mean measured distance. Its effectiveness and accessibility is true for the first 9 meters, but it is enough because it will be the most common distance from the beacon in small areas. In [21] the two-function, path loss model was proposed in which distance was estimated by different coefficients for near and far distances. In addition, only the nearest 3 beacons can be used for trilateration to reduce long distances from far beacons to minimize trilateration algorithm errors. Fig. 14 shows the correlation of distance estimation error by a model related to beacon RSSI value from Fig. 10 and the error growth presented on Fig. 13.

The distance estimation error is computed as follows:

$$e(\hat{d}) = | d_{real} - \hat{d}_{estimated} | \tag{16}$$

$$d_{real} = d(B,P) = \sqrt{(x_b - x_p)^2 + (y_b - y_p)^2 + (z_b - z_p)^2} \tag{17}$$

where:

B – the beacon position,

P – the measurement point.

Another important data processing has been applied, that is, a filter for input data. The survey indicated whether the processing was required and what kind of processing was preferred. Model (1) for distance estimation was used. The following methods of filtering data (all collected samples) in order to obtain a single $RSSI_{(b,\ p)}$ reference value for beacon b in a specific point p were applied:

1. The average value for all (n) samples acquired at the specific point p over distance up to 20m (step 1m);

$$RSSI_{avg(b,p)} = \frac{1}{n}\sum_{i=1}^{n} RSSI_{(p,b,i)} \tag{18}$$

2. The median value for all samples acquired at the specific point over distance up to 20m (step 1m);

$$RSSI_{med(b,p)} = RSSI_{\left(p,\frac{n+1}{2}\right)} \quad for\ n\ odd$$

$$RSSI_{med(b,p)} = \frac{1}{2}\left(RSSI_{\left(p,b,\frac{n}{2}\right)} + RSSI_{\left(p,b,\frac{n}{2}+1\right)}\right) \quad for\ n\ even \tag{19}$$

3. The average value after applying moving average filter with window size w = 6;

$$RSSI_{avg6(b,p)} = \frac{1}{n-w}\sum_{i=1}^{n-w}\sum_{k=i}^{w} RSSI_{(p,b,k)} \tag{20}$$

4. The average value after deleting 50% samples of the input data at the specific point. The subset contains acquired RSSI with the smallest error with respect to the **average** of all data. (in short: Average of 50% near Average);

4.1. Calculate the average RSSI value (see point. 1). Mark this value as reference $RSSI_{avgref}$:

$$RSSI_{avgref} = RSSI_{avg(b,p)}$$

4.2. Create the empty final set F of filtered $RSSI_{(b,\ p)}$ values. Set the final set F count FC to 0.

4.3. Make k the subsets of values (series of intervals) B_k of size, w that contains $RSSI_{(b,\ p,\ n)}$ values as follows:

$$RSSI_{(b,p,\min)} = \min(RSSI_{(b,p,1)}, RSSI_{(b,p,2)}, ..., RSSI_{(b,p,n)}) \tag{21a}$$

$$RSSI_{(b,p,\max)} = \max(RSSI_{(b,p,1)}, RSSI_{(b,p,2)}, ..., RSSI_{(b,p,n)}) \tag{20b}$$

$$w = \frac{RSSI_{(b,p,\max)} - RSSI_{(b,p,\min)}}{k} \tag{21c}$$

$$\forall_{B_m, m=1..k} \exists RSSI_{(b,p,n)} \Leftrightarrow ((m-1)\cdot w + RSSI_{(b,p,\min)})) \le RSSI_{(b,p,n)} < (m\cdot w + RSSI_{(b,p,\min)}) \tag{22}$$

Subsets (bins width) are sorted ascending by its containing values.

$$\forall_{B_m, m=2..k-1} \forall_{RSSI_m \in B_m} RSSI_{m-1} < RSSI_m < RSSI_{m+1} \tag{23}$$

Each $RSSI_{(b,\ p,\ n)}$ value is now assigned to the exactly one of the B_k subset. Each B_k subset contains BC_k values:

$$BC_k = | B_k |$$

4.4. Set i = 0 (step counter); Match the reference $RSSI_{ref}$ value with one subset (such as one of the values in step 4.3)

and get its index denoted by *mref*. All values in B_{mref} subset are very close to the reference value.

4.5. Move all values from sets:

a. B_{mref} (if $i = 0$) – the center

b. B_{mref-i} (if $mref - i \geq 0$ and $i \neq 0$)

c. B_{mref+i} (if $mref + i \leq k$ and $i \neq 0$)

to the final *F* set and add their count to the *FC* if added.

4.6. If *F* set contains more than 50% values ($FC \geq 0.5n$), go to step 4.7, otherwise increment *i* (check), then go to step 4.5 (to take next left- and right-side subsets).

4.7. Make an average of values from set *F*:

$$RSSI_{avg50(b,p)} = \frac{1}{FC}\sum_{i=1}^{FC} RSSI_{(p,b,i)} \quad (24)$$

5. The average value after deleting 50% samples of the input data at a specific point. The subset contains acquired RSSI with the smallest error with respect to the **median** of all data. (in short: Avg. of 50% near Median); Methodology:
The same as in 4), but $RSSI_{ref}$ is represented by the Median from RSSI (as in method 2) values rather than the Average.

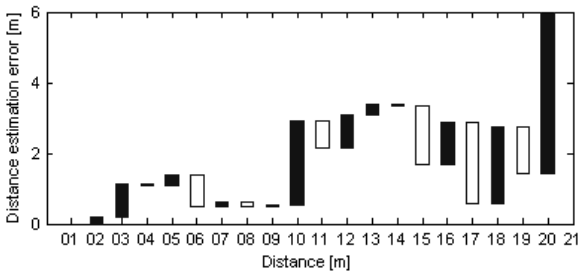

Fig. 15. Error of Distance estimation by tuned model over the distance (Average method).

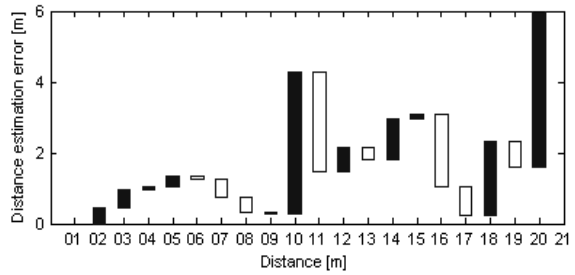

Fig. 16. Error of Distance estimation by tuned model over the distance (Avg of 50% hist. values near Avg).

The aforementioned techniques allow for obtaining a single RSSI value (reference value) at a specific distance from the beacon. The results of distance estimation using filtering data are shown in figures 15 and 16 and also in Table I.

TABLE I.
PATH-LOSS MODEL DISTANCES ESTIMATION ERROR FOR PROPOSED DATA PROCESSING METHODS

Method of transformation input data	**RSSI0 [dBm]**	**γ_{opt}**	**Avg. dist. estim. Error [m]**
Median	-57	-1.41279	2.6533
Average	-56.87	-1.33379	2.4914
Moving average (window size 6)	-56.83	-1.41455	2.4696
Avg. of 50% near Avg.	-56.79	-1.33330	2.2703
Avg. of 50% near Median	-56.79	-1.41982	2.6799

The candles plots represent the variation of error changes over the distance. The average value from the subset of 50% values that are near average value results in less standard deviation and less error dynamics. The average distance estimation error is 1.09m for distance 0-9m and equals to 4.05m for higher distance from the source; overall, the error is equal to 1.75m for 1-20m. For both examples (Fig. 15, 16), the model is accurate enough in the range 0-9 m, while over 10 m, dynamics of estimation error increases. It means the model proposed can be investigated and applied in the near range distance.

Rejecting 50% values from histogram that are not close to average reduces standard deviation and final distance estimation error. In case of median value distance estimation for the assumed model, it is less accurate because of the sorting phase while significant values can be shifted from the center.

IV. EXPERIMENTAL RESULTS

The tuned model was applied to surveyed roadmap to compare estimated distances and positions after trilatration. The reference value $RSSI_0$ was obtained at d_0=1.532m distance. For each radiomap point, the *RSSI* aggregate based on 100 samples was calculated by using different methods of filtering and aggregating to a single value presented in section 5. Moreover, for all the above aggregating methods, the tuned model was recalculated using the same method to obtain new γ_{opt} value. The average distance estimation error was calculated as an absolute value of difference from model estimation and real distance (15), which is presented in Table II. The error is also presented as heat map in Fig. 17.

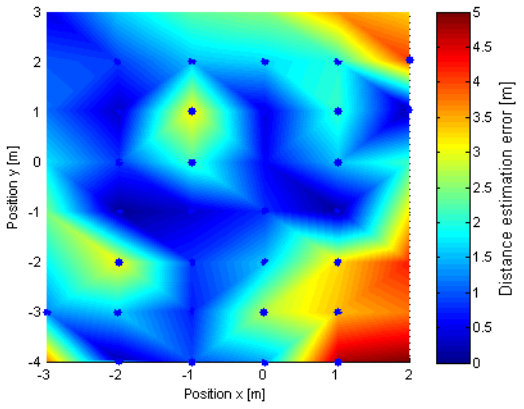

Fig. 17. Distance estimation error for trilateration algorithms considering three the nearest beacons by estimated distance.

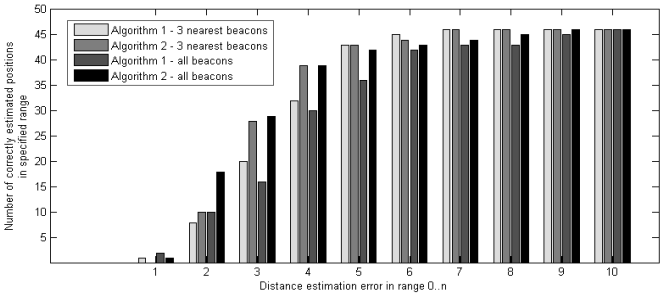

Fig. 18. Distribution of position estimation errors computed by algorithms comparing the number of beaons considered while trilateration.

The trilateration algorithms (III.A. and III.B.) were applied in the exemplary hall (5m x 7m, most distances up to 9m), that is, algorithms for all visible beacons and for 3 with the highest RSSI at the present position were evaluated. Cumulative number of correct positioning with respect to the distance from the real location is presented in Fig. 18. The average positioning error in the range 0-9m for both algorithms is depicted in Table II.

TABLE II.
TRILATERATION ALGORITHMS – NUMBER OF INPUT BEACONS COMPARISON – RESULTS

Selected beacons	Total Avg. positioning error [m]	
	Alg. 3.A.	Alg. 3.B.
All visible beacons	3.2524	2.3150
3 the nearest beacons (distance is estimated)	2.7658	2.4495

All visible beacons are ascending, sorted with respect to estimated distances (based on RSSI) at a current position of mobile device. Obtained results (see Table II) showed better results when compared to algorithm 3.B by examining the 3 nearest (chosen based on the estimated distances) beacons for first algorithm (3.A). However, algorithm 2 (3.B), where all visible beacons were taken into account achieved the best average result and its distribution is narrow, right skewed and concentrated near minimum error (Fig. 18). It is more tolerant for errors. In further considerations, the second algorithm (3.B) with only 3 beacons was used because accuracy of 0.12m costs two more beacons.

Analyzing Table I (and Table III), it can be said that data preprocessing (see explanation below in Table III) indicated lower distance estimation error: about 0.04m which is only ~2%. It is doubtful whether model calibration for specific metric is needed. The results of estimating distance for radiomap (Table III) are better than distance estimation presented for the tuned model (Table I) because almost all distances in radiomap are in the range 0-9 m, where estimation error is about 1m for tuned model (Fig. 13). The right most colomn shows average distance estimation error for (RSSI0 calculated by indicated algorithm), γ_{opt} calculated by median (*) (check) and indicated method (#), respectively.

TABLE III.
PATH-LOSS MODEL DISTANCES AND POSITIONS ESTIMATION ERROR – RESULTS

Processing method	$RSSI_0$ [dBm]	γ_{opt}	Avg. distance estim. error [m]
Median	-81.00	-1.33379	2.20171
Average	-81.45	-1.33379*) -1.41279#)	2.10073*) 2.06802#)
Moving average (window size 6)	-81.28	-1.33379*) -1.41455#)	2.11107*) 2.06361#)
Avg of 50% near Avg	-80.90	-1.33379*) -1.41982#)	2.23454*) 2.23513#)
Avg of 50% near Median	-81.56	-1.33379*) -1.33330#)	2.15095*) 2.09592#)

The symbols: #) denotes that the path-loss log model which was built with data processed by the indicated method; *) represents the model calculation with the use of median.

Estimated distances were utilized as input parameters for trilateration algorithms to compute the final position. The average error of all points in a whole radiomap was measured by comparing the estimated position and real radiomap position. Results are presented in Table IV.

Second algorithm (3.B) achieved better results. In each case, the effectiveness of estimating position is strictly related to the quality of input data, the smaller the distance estimation error using filtering method, the greater the precision of position estimation achieved. Average-based filtering gives surprisingly good results. It was proven that the filtering methods may give better results than median preprocessing, while the second approach to compute metric is less time and memory consuming. In addition, the error of distance estimation using the average of 50% data close to the average value which reduces the standard deviation of estimated distance significantly (Table I and Table III) have no positive effect on trilateration algorithms results.

TABLE IV.
FINAL POSITION ESTIMATES AND ERRORS

Method of transformation input data	$RSSI_0$ [dBm]	γ_{opt}	Avg. position error after trilateration [m]	
			Alg. 3.A.	Alg. 3.B.
Median	-81.00	-1.33379 n/a	2.90381	2.81877
Average	-81.45	-1.33379*) -1.41279#)	2.76580*) 2.73706#)	2.44952*) 2.44984#)
Moving average (window size 6)	-81.28	-1.33379*) -1.41455#)	2.78216*) 2.74580#)	2.45469*) 2.44152#)
Avg of 50% near Avg.	-80.90	-1.33379*) -1.41982#)	2.93677*) 2.89945#)	2.58144*) 2.58771#)
Avg of 50% near Median	-81.56	-1.33379*) -1.33330#)	3.02006*) 3.02047#)	2.65461*) 2.65490#)

The symbols: #) denotes that the path-loss log model has been built with data processed by the indicated method; *) represents the model calculation with the use of median.

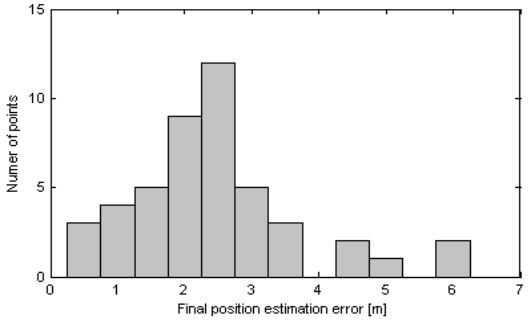

Fig. 19. Final position estimation error for whole radiomap.

Most of final position estimation errors after trilateration using the second algorithm (3.B)are less than 2.5m (60.87%), what is presented in fig. 19.

V. CONCLUSION

Bluetooth Low Energy and iBeacon standard opened a novel way to build low-power based positioning techniques. Obtained RSSI can be used for the estimation of device positioning but the preprocessing and good path-loss model is required. Distance estimation model gives more information than standard API's defined in iBeacon standard, which returns

only proximity range name if the object is immediate, near or far away (without estimating distance as a value). BLE is widely supported on devices so it can be utilized to customer's waypath or shop indoor segments tracking.

The proposed path-loss distance model is a good solution to determine device distance from the beacon in a range 1 – 9 m, because 1.09 m error is acceptable (Fig. 15, 16). For surveyed radiomap in room (Fig. 9), almost all distances are in the range 1 – 9 m which mean that estimated distances can be used as input of trilateration algorithms. The standard deviation of surveyed samples does not depend on distance from the beacon. Research proved that the wave multipath, interferation, diffraction has an impact on the RSSI distribution [9], especially, the human body absorbs the signal strength what should be included while determining position. Samples distribution are not Gaussian in all surveyed points. Filtering data for assumed path-loss model has no significant impact (Table IV) on the final position but other advanced methods may improve accuracy significantly. After trilateration, the positions with average error 2.45m (Table IV) was achieved.

In positioning context, the better results can be achieved by correlating RSSI's with accelerometer, gyroscope and other sensors. Another solution is to use more sophisticated metrics than Euclidean, such as: excluding zones where an object cannot move, restricting situations when objects moved back while accelerometer measurements does not notice this fact. Such problem must be under investigation in the near future.

REFERENCES

[1] A. Van Nieuwenhuyse, L. De Strycker, N. Stevens, J.-P. Goemaere, and B. Nauwelaers, "Analysis of the Realistic Resolution with Angle of Arrival for Indoor Positioning:," *International Journal of Handheld Computing Research*, vol. 4, no. 2, pp. 1–16, 32 2013.

[2] K. D'Hoe, G. Ottoy, J.-P. Goemaere, and L. De STRYCKER, "Indoor Room Location Estimation," *Advances in Electrical and Computer Engineering*, vol. 8, no. 2, pp. 78–81, 2008.

[3] A. H. Sayed, A. Tarighat, and N. Khajehnouri, "Network-based wireless location: challenges faced in developing techniques for accurate wireless location information," *IEEE Signal Processing Magazine*, vol. 22, no. 4, pp. 24–40, Jul. 2005.

[4] H. Liu, H. Darabi, P. Banerjee, and J. Liu, "Survey of Wireless Indoor Positioning Techniques and Systems," *IEEE Transactions on Systems, Man and Cybernetics, Part C (Applications and Reviews)*, vol. 37, no. 6, pp. 1067–1080, Nov. 2007.

[5] Z. M. Saric, D. D. Kukolj, and N. D. Teslic, "Acoustic Source Localization in Wireless Sensor Network," *Circuits, Systems and Signal Processing*, vol. 29, no. 5, pp. 837–856, Oct. 2010.

[6] A. K. M. M. Hossain and W.-S. Soh, "A Comprehensive Study of Bluetooth Signal Parameters for Localization," 2007, pp. 1–5.

[7] Educational Details: Mtech II year NIELIT Aurangabad, N. Allurwar, B. Nawale, and S. Patel, "Beacon for Proximity Target Marketing," *International Journal Of Engineering And Computer Science*, May 2016.

[8] M. Botta and M. Simek, "Adaptive Distance Estimation Based on RSSI in 802.15.4 Network," *Radioengineering*, vol. 22, no. 4, pp. 1162–1168, Dec. 2013.

[9] A. Heinemann, A. Gavriilidis, T. Sablik, C. Stahlschmidt, J. Velten, and A. Kummert, "RSSI-Based Real-Time Indoor Positioning Using ZigBee Technology for Security Applications," in *Multimedia Communications, Services and Security*, vol. 429, A. Dziech and A. Czyżewski, Eds. Cham: Springer International Publishing, 2014, pp. 83–95.

[10] A. T. Parameswaran, M. I. Husain, and S. Upadhyaya, "Is RSSI a reliable parameter in sensor localization algorithms: An experimental study," presented at the Field Failure Data Analysis Workshop (F2DA09), New York, 2009.

[11] M. S. Gast, *Building applications with iBeacon: [proximity and location services with Bluetooth Low Energy]*, 1. Aufl. Beijing: O'Reilly, 2015.

[12] *Beacon technologies: the hitchhiker's guide to the Beacosystem*. New York, NY: Springer Science+Business Media, 2016.

[13] Atreyi Bose and Chuan Heng Foh, "A practical path loss model for indoor WiFi positioning enhancement," 2007, pp. 1–5.

[14] A. Goldsmith, *Wireless Communications*. Cambridge: Cambridge University Press, 2005.

[15] T. S. Rappaport, *Wireless communications: principles and practice*, 2nd ed. Upper Saddle River, N.J: Prentice Hall PTR, 2002.

[16] M. Alshami, T. Arslan, J. Thompson, and A. T. Erdogan, "Frequency analysis of path loss models on WIMAX," 2011, pp. 1–6.

[17] Ł. Chruszczyk, A. Zając, and D. Grzechca, "Comparison of 2.4 and 5 GHz WLAN Network for Purpose of Indoor and Outdoor Location," *International Journal of Electronics and Telecommunications*, vol. 62, no. 1, Jan. 2016.

[18] P. Gilski and J. Stefański, "Survey of Radio Navigation Systems," *International Journal of Electronics and Telecommunications*, vol. 61, no. 1, Jan. 2015.

[19] Dai Lu and D. Rutledge, "Investigation of indoor radio channels from 2.4 GHz to 24 GHz," 2003, vol. 2, pp. 134–137.

[20] G. Luo, "Wavelet Notch Filter Design of Spread-Spectrum Communication Systems for High-Precision Wireless Positioning," *Circuits, Systems, and Signal Processing*, vol. 31, no. 2, pp. 651–668, Apr. 2012.

[21] V. S. Abhayawardhana, I. J. Wassell, D. Crosby, M. P. Sellars, and M. G. Brown, "Comparison of Empirical Propagation Path Loss Models for Fixed Wireless Access Systems," 2005, vol. 1, pp. 73–77.